WEP Warwick Evans Publishing

International Journal of Natural Resources and Environmental Studies

ISSN: 3006-2012 (Print), ISSN: 3006-0834 (Online) | Volume 2, Number 1, Year 2024
DOI: https://doi.org/10.62051/ijnres.v2n1.18
Journal homepage: https://wepub.org/index.php/IJNRES/index

Smooth Transition Control Strategy for Operation Modes of Optical Storage Microgrid based on VSG

Guiping Huang[1, *], Yan Xia[1], Kai Yang[1]

[1] School of Automation and Information Engineering, Sichuan University of Science & Engineering, Zigong 643000, China

*Corresponding Author: Guiping Huang

ABSTRACT

Addressing the challenge of suppressing voltage and frequency oscillations during mode transitions and achieving smooth transitions between grid-connected and islanded operation modes in peer-to-peer structured optical storage microgrids, is an urgent technical issue. This paper proposes a control strategy for smooth mode transitions based on numerical soft starters, focusing on the dynamic characteristics of voltage and frequency in optical storage microgrids during grid-connected and islanded operation modes. The numerical soft starter smoothens the input reference value of the current inner loop, reducing the impact of transient surge current on the current inner loop during transitions, thus ensuring the oscillations of bus voltage and frequency during microgrid mode transitions. In islanded operation mode, a VSG control strategy is introduced by constructing a small signal model to analyze the frequency response characteristics of the system under different inertia and damping characteristics, setting appropriate control parameters to provide strong frequency support for the system during islanded operation. Finally, an optical storage microgrid system is established using Matlab/Simulink to conduct simulation experiments under conditions such as grid-connected/islanded mode transitions, load fluctuations, and sudden changes in photovoltaic output power, validating the effectiveness of the proposed smoothing strategy.

KEYWORDS

Optical storage microgrid. Peer-to-peer structure. VSG control. Smooth transition.

1. INTRODUCTION

As the global energy and environmental crises intensify, the proportion of renewable energy sources such as solar and wind power in the power system continues to rise. Microgrids, by integrating distributed energy sources such as photovoltaics and wind power, energy storage systems, power electronic devices, local loads, and regulatory dispatch systems, can operate either in parallel with the main grid or switch to islanded operation mode according to scheduling plans or in the event of unplanned faults. They provide voltage and frequency support for local loads, ensuring the stable operation of these loads and demonstrating high power supply security and reliability[1]. The operational capability of microgrids in grid-connected and islanded operation modes is crucial for providing power support. Issues such as transient impacts and power imbalances during the switching process directly affect the safety and stability of the power system[2]. Therefore, smooth transition strategies become a key technology for microgrids to transition smoothly between grid-connected and islanded operation modes.

Currently, significant progress has been made in both domestic and international research on smooth transition technologies for microgrids. Among these, the control strategies for grid-connected

inverters mainly include master-slave control and peer-to-peer control. Microgrids based on the master-slave structure typically employ PQ control during grid-connected operation, directly controlling the grid current, while V/F control is used during islanded operation to provide voltage and frequency references for other inverters. Reference [3] utilizes phase-locked loop (PLL) technology to achieve smooth transitions between grid-connected and islanded operation modes. However, PLL involves complex coordinate transformations, increasing computational complexity and impacting control precision. Reference [4], on the other hand, achieves smooth transitions between grid-connected and islanded modes by controlling current loop outputs through setting saturation limits. Nevertheless, saturation limits may introduce significant disturbances during the transition process, affecting the selection of controller parameters. Building upon these works, Reference [5] introduces a pre-synchronization controller into the transition control, alleviating frequency oscillations during the transition process and achieving flexible switching. However, to ensure stable operation of microgrids based on master-slave control, controllable power sources with sufficient available capacity, such as diesel generators or micro-gas turbines, are required as grid power sources[6]. This contradicts the future development trend of power systems based on high-penetration renewable energy sources. Therefore, it is necessary to research microgrid control strategies based on peer-to-peer control. Such strategies can provide energy support for local loads during microgrid islanded operation while mitigating issues caused by insufficient system inertia and damping components due to traditional generator unit shortages.

Peer-to-peer control adjusts the voltage and frequency of microgrids by simulating the droop characteristics of generators, and in a grid-connected system, it can achieve power distribution and energy support among various distributed power sources without the need to consider interconnection signals. However, due to limitations such as line impedance constraints[7] and parallel circulating currents[8] in traditional droop control, many improvements are needed to enhance its mode switching capabilities. On the other hand, VSG control strategies draw inspiration from the operation principles of synchronous generators, endowing microgrids with the inertia and damping characteristics of synchronous machines, thereby improving the disturbance rejection properties of inverters. Reference [9] proposes a smooth transition control strategy based on pre-synchronization VSG, combining phase synchronization and voltage amplitude synchronization, addressing the shortcomings of VSG control in low-voltage ride-through control. References [10] and [11] analyze the basic structure and control methods of VSG and propose a parallel switching control strategy based on controller state tracking, suppressing oscillations in microgrid bus voltage and current distortion during the switching process.

Addressing the aforementioned issues, this paper focuses on optical storage AC/DC microgrids. It analyzes the operational modes of microgrids and proposes a smooth transition control strategy based on VSG control and numerical soft starters. The VSG control strategy enhances the power and frequency support capability of optical storage systems during islanded operation mode, while the numerical soft starters reduce transient surge currents during mode transitions, enabling smooth transitions between operational modes of optical storage microgrids. The effectiveness of the proposed smooth transition control strategy is validated through simulation using Matlab/Simulink.

2. DISTRIBUTED OPTICAL STORAGE AC/DC MICROGRID

The topology of a distributed optical storage AC/DC microgrid based on a master-slave structure is illustrated in Figure 1. The main components of the system include distributed photovoltaic (PV) generation systems, energy storage systems, AC load units, Point of Common Coupling (PCC), and corresponding control strategies. The PV generation system is connected to the 600V microgrid AC side via a boost circuit and DC/AC inverter. The energy storage system is connected to the 600V microgrid AC side via an energy storage inverter. Different operational modes of the microgrid under various conditions lead to different control strategies for each distributed power source.

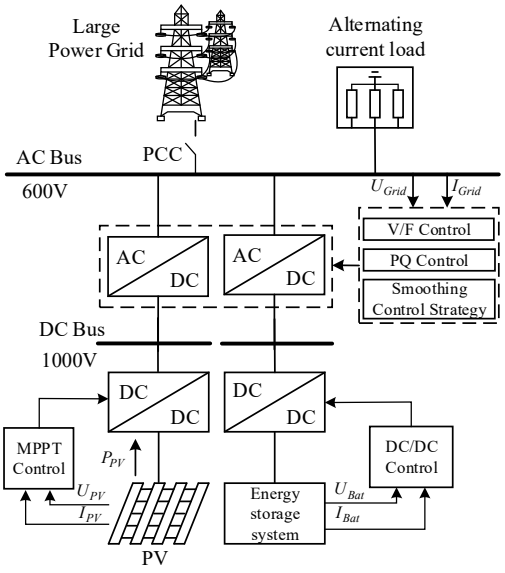

Figure 1. Distributed optical storage AC-DC microgrid topology.

3. STRUCTURE AND CONTROL OF ENERGY STORAGE INVERTER

The primary control topology of the energy storage inverter is depicted in Figure 2. According to grid dispatch schedules or unplanned islanding faults, the PCC is either connected or disconnected to achieve the transition of microgrid operation modes. When the PCC is connected, the microgrid operates in grid-connected mode. The energy storage inverter adopts a PQ control strategy, providing power support to the main grid in strong grid conditions, maximizing the utilization of new energy resources. When the PCC is disconnected, the microgrid operates in islanded mode. It adopts a VSG control strategy, supplying electric energy to the local loads of the microgrid and providing voltage and frequency support to other distributed power sources.

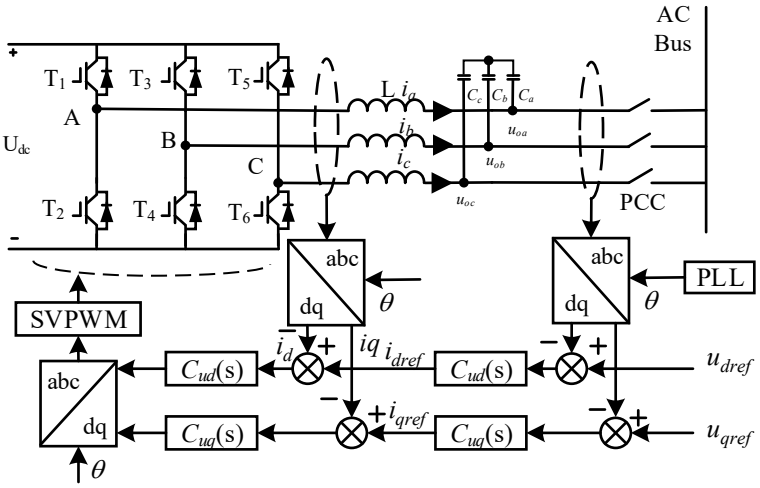

Figure 2. Control topology of energy storage converter.

3.1. PQ Control Strategy in Grid-Connected Mode

When the microgrid is connected and operates in parallel with the main grid, the energy storage inverter adopts a PQ control strategy. The reference values for power control loops are set according to the power output requirements. In strong grid conditions, this control strategy not only maximizes the utilization of renewable energy sources but also provides reliable power supply to the main grid.

The PQ control primarily consists of an outer power loop and an inner current loop. The outer power loop decouples the active power and reactive power control by analyzing the power from the main grid. In grid-connected mode, the active power and reactive power can be represented as:

$$\begin{cases} P = U_d I_d + U_q I_q \\ Q = U_q I_d - U_d i_q \end{cases} \tag{1}$$

When selecting the d-axis to be aligned with the A-phase voltage vector, the d-axis voltage component Ud can be regarded as constant, with the q-axis voltage component Uq=0. Hence, the above equation can be simplified as:

$$\begin{cases} P = U_d I_d \\ Q = -U_d i_q \end{cases} \tag{2}$$

The power outer-loop equation for the PQ control strategy is given by equation (3), while the current inner-loop equation is represented by equation (4).

$$\begin{cases} i_{dref} = \left(K_P + \dfrac{K_I}{s} \right) \left(P_{ref} - P \right) \\ i_{qref} = \left(K_P + \dfrac{K_I}{s} \right) \left(Q_{ref} - Q \right) \end{cases} \tag{3}$$

$$\begin{cases} u_{sd} = \left(K_p + \dfrac{K_I}{s} \right) \left(i_{dref} - i_d \right) - L\omega i_q + u_{od} \\ u_{sq} = \left(K_p + \dfrac{K_I}{s} \right) \left(i_{qref} - i_q \right) + L\omega i_d + u_{oq} \end{cases} \tag{4}$$

According to the above equations, the schematic diagram for the PQ control principle is depicted in Figure 3.

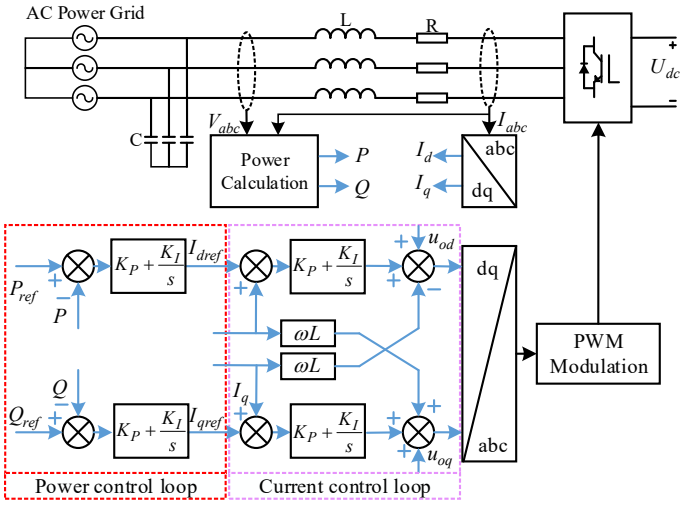

Figure 3. PQ control principle block diagram.

3.2. VSG Control Strategy in Islanded Mode

Based on the traditional droop characteristics of synchronous generators and to avoid the complex electromagnetic coupling issues associated with synchronous generators, a second-order model is simulated. Drawing from the rotor motion equation and electromagnetic equation, a VSG control strategy is proposed. This aims to address the lack of rotating inertia and damping components in

power systems with high penetration of renewable energy sources. The strategy is intended to enhance the voltage and frequency support capability of the system during islanded operation.

3.2.1. VSG Control Principle

Drawing inspiration from the second-order control model and implicit pole number 1 synchronous generator mathematical model, the mechanical equation representation of VSG is proposed as follows:

$$\begin{cases} J\dfrac{d\omega}{dt}=\dfrac{P_{ref}-P}{\omega_0}-T_d=T_m-T_e-D(\omega-\omega_0) \\ \dfrac{d\delta}{dt}=\omega\text{-}\omega_0 \end{cases} \tag{5}$$

Where T_m represents the virtual mechanical torque of the VSG; T_e denotes its virtual electromagnetic torque; J signifies the virtual moment of inertia; ω represents the virtual angular frequency of the VSG; with ω_0 being its rated angular frequency; D represents the damping coefficient; δ denotes the power angle; P_{ref} and P respectively represent the mechanical power and electromagnetic power.

Drawing from the traditional Automatic Frequency Regulator (AFR) of synchronous generators, a primary frequency regulator for the VSG can be constructed. The mechanical deviation command ΔT can be expressed as:

$$\Delta T=P_T-P_{ref}=k_\omega(\omega_0-\omega) \tag{6}$$

In the equation: k_ω represents the droop control coefficient; P_T denotes the mechanical power. Substituting equation (6) into equation (5), the active power control loop of the VSG can be expressed as equation (7), and based on this, the control principle diagram of the VSG active power control loop is constructed as shown in Figure 4.

$$\frac{P_{ref}+k_p\left(\omega_{ref}-\omega\right)-P_e}{\omega_0}=J\frac{d\omega}{dt}+D\left(\omega-\omega_0\right) \tag{7}$$

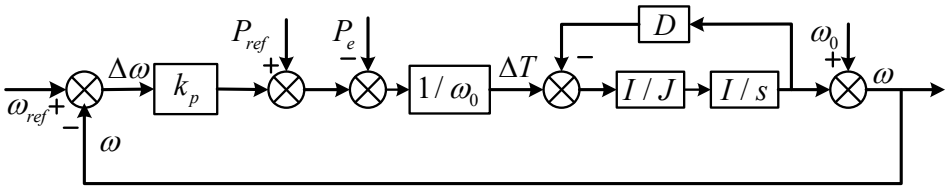

Figure 4. VSG active power control loop schematic diagram.

Drawing from the traditional method of regulating reactive power output and terminal voltage of synchronous generators using excitation adjustment, based on the reactive power-voltage droop control, the primary voltage control equation for VSG can be expressed as follows:

$$E=\left[E_N+k_V\left(Q_{ref}-Q\right)-E_m\right]\left(k_p+\frac{k_1}{s}\right) \tag{8}$$

In the equation, Q_{ref} represents the reactive power setpoint; Q denotes the actual output reactive power of the inverter; k_V represents the voltage deviation coefficient; E_N represents the rated voltage reference value; E represents the calculated voltage reference value; E_m represents the terminal voltage magnitude. Based on the above equation, the primary voltage control principle diagram for VSG can be constructed as shown in the following figure:

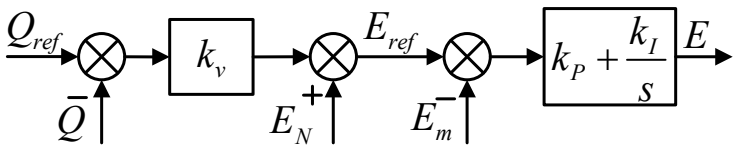

Figure 5. VSG primary voltage regulation control principle block diagram.

3.2.2. Impact of Parameter Settings on the Frequency Response Characteristics of VSG

In terms of the control performance of energy storage inverters employing VSG, a larger moment of inertia J suppresses fluctuations in the frequency of the AC bus system when loads are frequently switched. This enhances the system's frequency support capability. However, if the moment of inertia J is set improperly, it may lead to system frequency oscillations, thereby affecting the stable operation of the system. Additionally, the damping component of VSG control enables the energy storage system to quickly recover the system frequency when subjected to certain external disturbances. If the damping component D is set improperly, it may affect the system's response time, thereby reducing the dynamic performance of VSG control. Therefore, setting the moment of inertia J and damping component D of VSG reasonably can enhance the frequency support capability of VSG and optimize the system's dynamic response performance.

Considering VSG as an ideal controllable voltage source connected to an infinite grid through a transmission line, the active power and reactive power output can be obtained using the calculation method of apparent power, as expressed by the following equations:

$$P_A = \frac{V_A}{R^2 + X^2}\left[R\left(V_A - V_B \cos\delta\right) + XV_B \sin\delta\right] \tag{9}$$

$$Q_A = \frac{V_A}{R^2 + X^2}\left[-RV_B \sin\delta + X\left(V_A - V_B \cos\delta\right)\right] \tag{10}$$

In the equation, V_A and V_B represent the voltage magnitudes of VSG and the grid, respectively, while δ corresponds to the phase difference between the two voltage vectors. R+jX denotes the impedance of the transmission line. In power systems, the impedance of high-voltage and medium-voltage systems' lines is typically inductive, hence neglecting the resistive part of the line impedance. As the power angle δ in the line is typically very small, we assume $\sin\delta \approx \delta$ and $\cos\delta \approx 1$. Simplifying the above equation, we obtain equation (11):

$$\begin{cases} P_A \approx \dfrac{V_A}{X}\left(V_B \sin\delta\right) \Rightarrow \delta \approx \dfrac{XP_A}{V_A V_B} \\ Q_A \approx \dfrac{V_A}{X}\left(V_A - V_B \cos\delta\right) \Rightarrow V_A - V_B \approx \dfrac{XQ_A}{V_A} \end{cases} \tag{11}$$

Based on equation (11) and equation (7), the small-signal model of VSG can be constructed as follows:

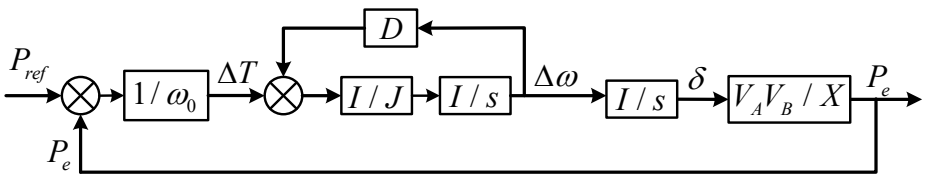

Figure 6. VSG small signal model.

According to the above equation, the closed-loop transfer function of VSG can be derived as shown in equation (12), where the natural oscillation angular frequency and damping ratio are represented as follows:

$$G(S)=\frac{\frac{V_A V_B}{J\omega_0 X}}{s^2+\frac{D}{J}s+\frac{V_A V_B}{J\omega_0 X}} \tag{12}$$

$$\begin{cases}\omega_n=\sqrt{\dfrac{V_A V_B}{J\omega_0 X}}\\ \xi=\dfrac{D}{2}\sqrt{\dfrac{\omega_0 X}{JV_A V_B}}\end{cases} \tag{13}$$

Based on equations (12) and (13), the frequency response characteristics of the active power control loop transfer function of VSG under different moments of inertia and damping components can be obtained from the input step response signal, as illustrated in Figure 7:

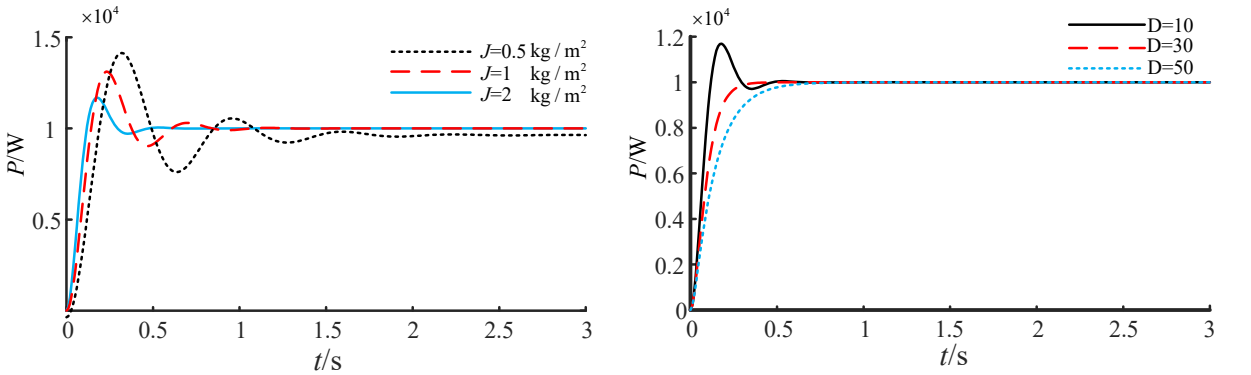

(a) D = 10, Step response corresponding to different parameters J (b) J = 0.5, Step response corresponding to different parameters D

Figure 7. Active power step response curve under different parameters.

From the above figure, it can be observed that as the moment of inertia J increases gradually, the natural oscillation angular frequency ω_n and damping ratio ζ of the second-order system decrease progressively, leading to more intense oscillations and longer stability time. Conversely, as the damping component D increases gradually, while the natural oscillation angular frequency ωn remains unchanged, the damping ratio ζ increases gradually. Consequently, the response curve becomes smoother, and the stability time decreases, resulting in a more stable system.

3.3. Seamless Switching Control Strategy for Grid-Connected/Islanded Operation Modes

Microgrids operate in two modes: grid-connected and islanded. To ensure stable and efficient operation under different conditions, it is necessary to address the challenges during the transition between grid-connected and islanded modes. During this transition, the grid-connected inverter experiences an instantaneous decay of grid power to zero, while the main control unit operates in PQ control mode, maintaining the active power reference value at the grid-connected reference value. This leads to power imbalances between the main control unit's output power and local loads, as well as fluctuations in microgrid AC voltage and frequency. Therefore, it is essential to study seamless switching strategies based on PQ control and VSG control. These strategies aim to enhance the

system's power and frequency support capabilities while achieving smooth transitions between grid-connected and islanded modes in photovoltaic and energy storage microgrids.

In response to the aforementioned issues and leveraging the technical characteristics of PQ control and VSG control, a parallel smooth switching control strategy based on numerical soft starters is proposed. This strategy involves running PQ control and VSG control strategies in parallel. Exploiting the similarity in the current inner-loop control structure of the two control methods, a soft starter is introduced to achieve smooth switching of currents between grid-connected and islanded operation modes for grid-connected inverters. The specific adjustment expression for the numerical soft starter is formulated as follows:

$$\begin{cases} id = i_{PQd} + \int_0^T \Delta i_{Ld} dt = i_{PQd} + \int_0^T \dfrac{i_{VSGd} - i_{PQd}}{T} dt \\ iq = i_{PQq} + \int_0^T \Delta i_{Lq} dt = i_{PQq} + \int_0^T \dfrac{i_{VSGq} - i_{PQq}}{T} dt \end{cases} \tag{14}$$

In the equation, T represents the ramp-up time from the initial value to the final value, and Δi denotes the step size.

From the above equation, it is evident that there are numerical differences between I_{PQ} and I_{VSG}. By considering I_{PQ} and I_{VSG} as the initial and final values of the soft starter, and adjusting them through the soft starter, I_{PQ} gradually transitions to I_{VSG}. This ensures smooth switching between grid-connected and islanded operation modes for the microgrid.

4. SIMULATION VERIFICATION AND ANALYSIS

To validate the effectiveness of the proposed strategies, a simulation platform for mode switching in photovoltaic and energy storage microgrids was built using MATLAB/Simulink, based on the topology depicted in Figure 1. The simulation duration was set to 4 seconds, with the following parameters: DC voltage of the photovoltaic and energy storage systems, U_{dc} = 800V; grid-side AC bus voltage, U_{Grid} = 600V; and system frequency of 60Hz. The main parameters of the VSG control system are listed in Table 1. During the simulation verification, the analysis primarily focuses on the challenging aspect of unplanned islanded operation in microgrids, followed by the validation of the effectiveness of the proposed grid-connected/islanded smooth switching control strategy. Figure 8 illustrates the output power of various distributed energy sources in the microgrid during the smooth switching between grid-connected and islanded operation modes.

Table 1. VSG main parameters of the control system.

VSG Control			
Parameter	Value	Parameter	Value
R_f /Ω	0.12	J /(kg·m^2)	0.5
L_f /mH	4.7	D /(N·m·s·rad^{-1})	10
C /μF	30	K_p	5000

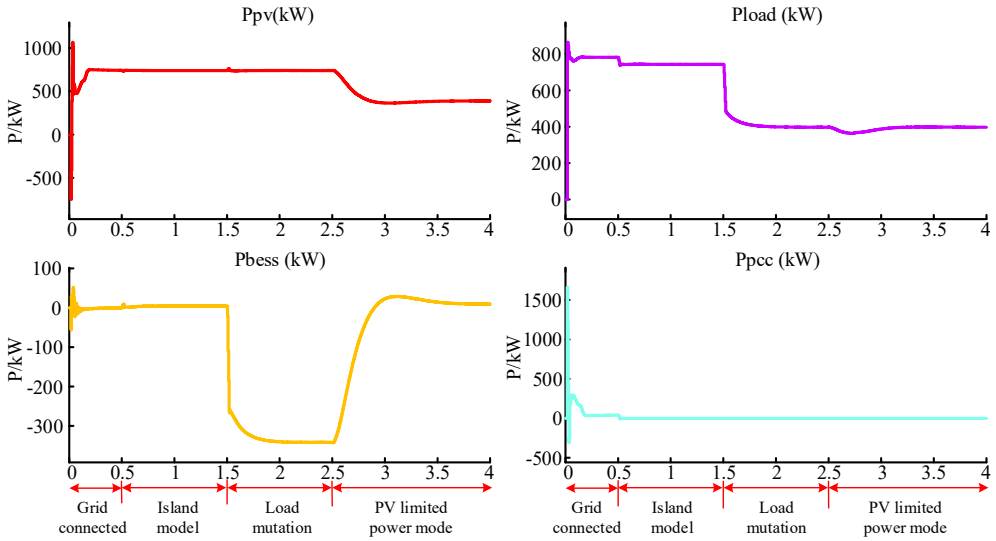

Figure 8. Simulation waveform of output power of each distributed power source in microgrid.

By comparing the simulated power results below, it can be visually observed that the microgrid operates in grid-connected mode before 0.5s and experiences an unplanned transition to islanded mode after 0.5s. The PV generation system continuously supplies power to the grid with an output power of 700 kW from 0s to 2.5s, providing power support to the local load. At 1.5s, the local load is reduced from 750 kW to 400 kW, and the energy storage system absorbs 350 kW of redundant power from the microgrid. At 2.5s, the dispatching system switches the PV system to power limiting mode based on the local load requirements, providing power equivalent to the load demand to the microgrid, while the energy storage system exits the charging mode. From the above analysis, it can be inferred that the microgrid employing the smooth switching strategy exhibits minimal power fluctuations during the transition from grid-connected mode to islanded mode. Additionally, the microgrid system utilizing VSG control effectively dampens power fluctuations during sudden changes in PV output and load power.

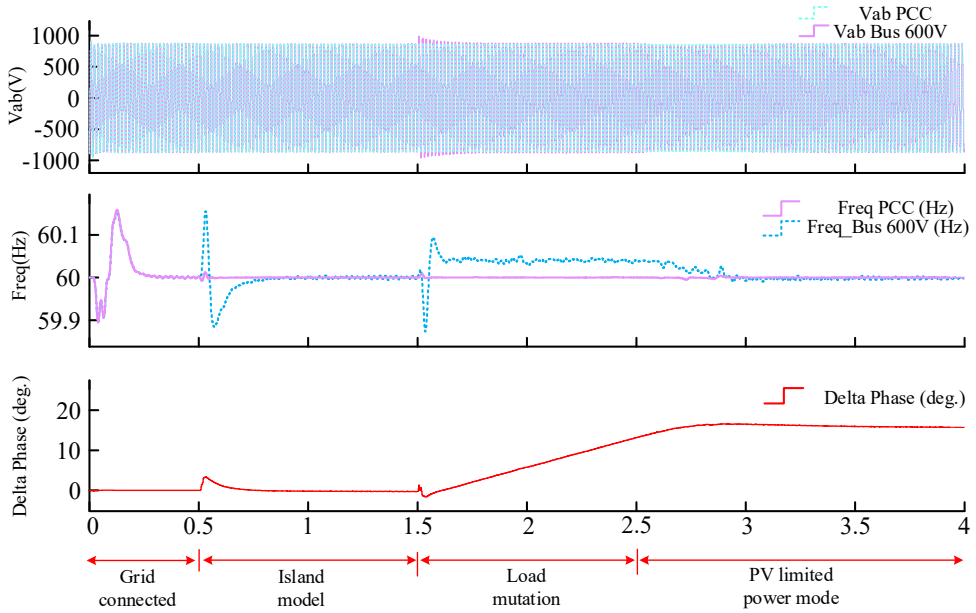

Figure 9. Simulation waveform of voltage and frequency between microgrid and main grid.

According to the comparison simulation curves of phase voltage and frequency between the microgrid and the main grid shown in Figure 9, it can be observed that, in terms of voltage magnitude and phase control, the phase voltages of the microgrid's AB phases exhibit only minor fluctuations after mode switching, with a phase deviation of 4 degrees. Moreover, the voltages quickly recover after 0.25s, maintaining stable voltage phase and magnitude. Regarding frequency control, the microgrid's frequency experiences slight oscillations before and after mode switching, with small overshoots and a maximum frequency deviation of 0.15Hz. The frequency rapidly recovers to 60Hz after 0.25s. Additionally, when the microgrid operates in islanded mode and experiences load or photovoltaic output power fluctuations, the grid-connected inverters employing VSG control can swiftly suppress frequency oscillations, ensuring the stability of the system's AC voltage and providing robust frequency support for islanded microgrid operation.

Based on the simulation analysis above, it is evident that the proposed smooth switching control strategy effectively suppresses power oscillations during grid-connected/islanded transitions. Furthermore, the microgrid's frequency and voltage can quickly recover during grid-connected/islanded transitions, achieving smooth transitions between microgrid operation modes.

5. CONCLUSIONS

This paper proposes a smooth switching strategy suitable for microgrids transitioning between grid-connected and islanded operation modes. A simulation model based on a peer-to-peer structured photovoltaic and energy storage microgrid was constructed using MATLAB/Simulink to validate the effectiveness of the proposed smooth switching strategy. The main contributions are summarized as follows:

1) Introducing VSG control strategy during islanded operation of the photovoltaic and energy storage microgrid. By analyzing the mathematical model of the virtual synchronous generator (VSG) and constructing a small-signal model of VSG, the impact of parameter settings on the system's frequency response characteristics was analyzed. This analysis helped determine the optimal parameter settings for the system, providing robust power and frequency support for the microgrid during islanded operation.

2) Introducing a numerical soft starter and proposing a smooth switching strategy for the microgrid between grid-connected and islanded operation modes. By utilizing the numerical soft starter to smoothly vary the reference setpoint in the current inner-loop control structure, the transient impact current caused by the switching of control structures was further reduced. This strategy achieved smooth transitions between grid-connected and islanded operation modes for the microgrid.

ACKNOWLEDGEMENTS

This project thanks to the support of Graduate Innovation Fund of Sichuan University of Light Chemical Technology with the number of Y2022119.

REFERENCES

[1] Xiao J, Wang P, Setyawan L. Implementation of multiple-slack-terminal DC microgrids for smooth transitions between grid-tied and islanded states[J]. IEEE Transactions on smart grid, 2015, 7(1): 273-281.

[2] Ansari S, Chandel A, Tariq M. A comprehensive review on power converters control and control strategies of AC/DC microgrid[J]. IEEE Access, 2020, 9: 17998-18015.

[3] CHEN Jingwen, ZHOU Yuan, Ll Xiaofei, et al. Hybridenergy storage control strategy of optical storage DCmicrogrid[J]. Smart Power, 2022, 50(1): 14-20.

[4] Ahmed I, Longting S, Xin C. A novel control scheme for microgrid inverters seamless transferring between grid-connected and islanding mode[C]//2017 China International Electrical and Energy Conference (CIEEC). IEEE, 2017: 75-80.

[5] Li H, Wang J, Hu A P, et al. Smooth switching control strategy for microgrid based on state following controller[C]//2018 2nd IEEE Conference on Energy Internet and Energy System Integration (EI2). IEEE, 2018: 1-4.

[6] Chen J, Chen X, Feng Z, et al. A control strategy of seamless transfer between grid-connected and islanding operation for microgrid[J]. Proc. CSEE, 2014, 34(19): 3089-3097.

[7] YUAN Chang, CONG Shixue, XU Yanhui. Overview on grid-connected inverter virtual impedance technology for microgrid[J]. Power System Protection and Control, 2017, 45(9): 144-154.

[8] FANG Hongwei, TAO Yue, XIAO Zhaoxia, et al. Robustcontrol and circulating current analysis for grid-connected parallel inverters[J]. Transactions of China Electrotechnical Society, 2017, 32(18): 248-258.

[9] Li Hua, Gao Huaizheng, Hao Yue, et al. Seamless switching control strategy for low voltage ride-through based on virtual synchronous generator[J]. Acta Energiae Solaris Sinica, 2021, 42(3): 114-120.

[10] WANG Gang, CHEN Xiaomin. Seamless switching control strategy of micro grid operation mode[J]. Journal of Henan Polytechnic University (Natural Science), 2018, 37(3): 93-100.

[11] Ma Hongtao, Zhou Bohao, He Yahui, et al. Seamless switching strategies for microgrid[J]. Smart Power, 2020, 48(5): 53-59.